

Neuroimaging Changes in Menkes Disease, Part 1

R. Manara, L. D'Agata, M.C. Rocco, R. Cusmai, E. Freri, L. Pinelli, F. Darra, E. Procopio, R. Mardari, C. Zanus, G. Di Rosa, C. Soddu, M. Severino, M. Ermani, D. Longo, S. Sartori, and the Menkes Working Group in the Italian Neuroimaging Network for Rare Diseases



ABSTRACT

SUMMARY: Menkes disease is a rare multisystem X-linked disorder of copper metabolism. Despite an early, severe, and progressive neurologic involvement, our knowledge of brain involvement remains unsatisfactory. The first part of this retrospective and review MR imaging study aims to define the frequency rate, timing, imaging features, and evolution of intracranial vascular and white matter changes. According to our analysis, striking but also poorly evolutive vascular abnormalities characterize the very early phases of disease. After the first months, myelination delay becomes evident, often in association with protean focal white matter lesions, some of which reveal an age-specific brain vulnerability. In later phases of the disease, concomitant progressive neurodegeneration might hinder the myelination progression. The currently enriched knowledge of neuroradiologic finding evolution provides valuable clues for early diagnosis, identifies possible MR imaging biomarkers of new treatment efficacy, and improves our comprehension of possible mechanisms of brain injury in Menkes disease.

ABBREVIATION: MD = Menkes disease

Menkes disease (MD) is a rare X-linked recessive disorder (Online Mendelian Inheritance in Man No. 309400; <http://omim.org/>)¹ due to mutations in the *ATP7A* gene (Xq13.2-q13.3), causing impaired absorption and cellular metabolism of

copper. The overall incidence of MD in Europe is reported to be 1 in 300,000 births.² Although the disease shows great clinical heterogeneity, most affected children present with early growth failure, hypothermia, failure to thrive, cutis laxa, and sparse, kinky hair (pili torti).³

The central nervous system is primarily involved, with severe cognitive and sensorimotor impairment, poor quality of life, and reduction in life expectancy. The spectrum of neurologic manifestations is strikingly wide; drug-resistant epilepsy appears in the first trimester of life, followed by regression of developmental milestones and progression to death in early childhood. Despite the wide phenotypic spectrum, some of the clinical features seem to present a recurrent age-related course, suggesting a possible concomitant role of brain maturation and age-related vulnerability to copper dysmetabolism. For example, epilepsy typically shows a 3-stage course: 1) focal seizures progressing to status epilepticus (<3 months), 2) epileptic spasms (6–11 months), and 3) multifocal seizures, tonic spasms, and myoclonus (20–25 months).⁴

The scarce neuropathologic data refer to the late phases of MD and point to diffuse cerebral and cerebellar atrophy, neuronal loss, gliosis within cortical and deep gray matter, loss of Purkinje cells, and cerebral white matter spongy changes along with loss of myelin sheaths and axons. Intracranial arteries appear thin-walled and strikingly tortuous.^{5,6}

In the past decades, MR imaging investigations have been routinely applied to in vivo intracranial changes in children with MD.

From the Neuroradiology (R. Manara, M.C.R.), Sezione di Neuroscienze, Medicine and Surgery Department, University of Salerno, Salerno, Italy; Department of Neuroscience (L.D.), University of Padova, Padova, Italy; Neurology Unit (R.C., D.L.), Department of Imaging, Bambino Gesù Children's Hospital IRCCS, Roma, Italy; Department of Pediatric Neuroscience (E.F.), Foundation I.R.C.C.S., Neurological Institute "C. Besta," Milano, Italy; Neuroradiology (L.P.), Section of Pediatric Neuroradiology, Department of Diagnostic Imaging ASST Spedali Civili, Brescia, Italy; Child Neuropsychiatry Unit (F.D.), Department of Life and Reproduction Sciences, University of Verona, Verona, Italy; Metabolic and Neuromuscular Unit (E.P.), Department of Neuroscience, Meyer Children Hospital, Firenze, Italy; Department of Neuroscience (R. Mardari, M.E.) and Pediatric Neurology and Neurophysiology Unit, Department of Woman and Child Health (S.S.), University Hospital of Padova, Padova, Italy; Institute for Maternal and Child Health (C.Z.), IRCCS "Burlo Garofolo," Trieste, Italy; Unit of Child Neurology and Psychiatry (G.D.R.), Department of Human Pathology of the Adult and Developmental Age, University Hospital of Messina, Messina, Italy; Ospedale Pediatrico Microcitemico "A. Cao" (C.S.), AOB Cagliari, Italy; and Neuroradiology Unit (M.S.), Istituto Giannina Gaslini, Genova, Italy.

Renzo Manara and Lauracarmen D'Agata contributed equally to the study and should be considered "first coauthors." Daniela Longo and Stefano Sartori should both be considered "senior coauthors."

Please address correspondence to Renzo Manara, MD, Neuroradiology, Sezione di Neuroscienze, Dept of Medicine and Surgery, University of Salerno, via S. Allende 1, Baronissi (SA), 84081 Italy; e-mail: rmanara@unisa.it

Indicates open access to non-subscribers at www.ajnr.org

Indicates article with supplemental on-line appendix and table.

Indicates article with supplemental on-line photos.

<http://dx.doi.org/10.3174/ajnr.A5186>

Table 1: Main data on intracranial vessel abnormalities in our MD sample and in 29 controls

	Children with MD	Controls
Sample size (No.)	26 Children	29 Children
Sex	25 M, 1 F	19 M, 10 F
Age at MRA (mean) (range) (mo)	14 ± 19 (2.2–86.7) ^a	11.5 ± 15 (0.2–82.3)
Tortuosity index (mean) (range)	0.41 ± 0.30 (0.07–1.08) ^a	0.07 ± 0.08 (0.01–0.31) ^b
Smoker score (mean) (range)	6.0 ± 1.3 (1–6) ^c	1.7 ± 0.7 (1–3) ^b

^a Calculated at first MRA in 15 children with MD.^b $P < .0001$.^c Calculated at first MRI in 26 children with MD.

Nonetheless, due to the rarity of the disease, imaging findings are also scarce, and our knowledge is based on scattered case reports and small case series. Increased intracranial vessel tortuosity, protean white matter signal abnormalities, transient temporal lobe changes, cerebral and cerebellar atrophy, basal ganglia anomalies, and subdural collections have been variably reported and associated with the clinical phenotype, leading to several and sometimes conflicting pathogenic hypotheses. So far, the frequency rate, precise characterization, timing, evolution, and likely pathogenesis of these neuroradiologic abnormalities remain unsatisfactorily understood.

The present large retrospective and review MR imaging study aimed to improve our knowledge of the intracranial involvement in Menkes disease to provide possible neuroradiologic biomarkers useful for diagnosis and follow-up. In particular, this first Part will address the intracranial vascular and white matter changes that might be observed during the course of MD.

MATERIALS AND METHODS

MR imaging and MRA findings of children with MD were retrospectively evaluated. Children were enrolled if they had a biochemically or genetically confirmed MD diagnosis and at least 1 MR imaging. All images were evaluated by 2 neuroradiologists with >15 years of experience in pediatric neuroradiology (R. Manara and D.L.), who were aware of the diagnosis but blinded to the clinical findings; discordant findings were discussed until consensus was reached.

The study included 40 MRIs (25 MRAs, all with the time-of-flight technique) of 26 children with MD (mean age at first MR image, 7.5 ± 5.9 months; range, 0.3–32.2 months; 1 female). Most studies were performed on 1.5T scanners (37/40) and included at least T2/FLAIR and T1-weighted images; DWI was available in 25/40 MRIs.

Intracranial Blood Vessel Evaluation

The qualitative evaluation of increased artery tortuosity was obtained from MRA or parenchymal T2-weighted images whenever angiography studies were not available. A semiquantitative evaluation of basilar artery dolichoectasia (Smoker score, see the On-line Appendix) was performed on axial T2 imaging. A quantitative evaluation of the basilar artery tortuosity was performed with commercially available software (syngo MultiModality Workplace; Siemens, Erlangen, Germany; see the On-line Appendix) in children with MD, who had time-of-flight 3D-MRA in a DICOM format (15 children; mean age, 14 ± 19 months; range, 2.2–86.7 months). Briefly, after recognizing the proximal and the distal end of the basilar

artery, the software allowed the measurement in millimeters of the effective length of the whole vessel (curved length) and the linear distance between the 2 extremes. A tortuosity index was subsequently calculated according to the formula: (Curved Length/Linear Length) – 1. The index is supposed to be zero if the 2 lengths are equal.

Basilar artery semiquantitative and quantitative evaluations were compared with those of 29 children without MD (Table 1) who underwent brain MR imaging and MRA for other indications.

The presence of stenosis or ectasia of the intracranial arteries was also evaluated on MRA studies, while the presence of venous sinus ectasia was assessed on parenchymal imaging.

White Matter Change Evaluation

Qualitative parenchymal evaluation was performed on all MRIs. Tumefactive lesions, centrum semiovale DWI hyperintense lesions, focal nontumefactive white matter lesions, and abnormal myelination, identified in previous publications, were recorded.

Literature Review

An extensive search was performed in all major data bases (Embase, Scopus, PubMed, Cochrane, and also www.google.com) with the following terms: “Menkes” and “brain MR imaging.” We included all articles reporting MR neuroimaging findings and age at MR imaging examination. From case descriptions or direct inspection of the published images, we investigated the presence/absence of abnormal findings on MR imaging/MRA. The lack of description combined with the impossibility of defining their presence/absence with the available published images was recorded as “not mentioned.” We also recorded any available information about the size, distribution, signal pattern, evolution, and proposed pathogenic hypothesis of white matter abnormalities described in children with MD.

Our literature review included 47 articles published between 1989 and August 2016 that are listed in the On-line Appendix.

Statistical Analysis

The variables with normal distribution were analyzed by using the Student *t* test, while for ordinal variables, the Mann-Whitney *U* test was used. Categorical variables were analyzed by using the χ^2 of the Pearson or the Fisher Exact test when required. The significance level was $P < .05$.

RESULTS

Table 2 summarizes the main features of our sample and of the literature data regarding children with MD who underwent brain MR imaging.

In our sample, 15 children with MD were alive at the time of the study; for the remaining 11 children, death occurred at 6.3 ± 4.6 years of age (range, 9 months to 17.5 years). All children showed severe early-onset neurodevelopmental impairment; most patients presented with epilepsy during the early phases of MD.

The On-line Table and Fig 1 summarize the main neuroradiologic findings of children with MD included in the study and in our literature review.

Intracranial Vessel Abnormalities

Literature Review. At the first MR imaging, increased artery tortuosity was present in 45/62 children with MD (73%), absent in 2, and not mentioned in 15. At follow-up, increased artery tortuosity was described in 14/23 (61%; in 4, the finding was not mentioned at the first examination), while in 9, it was not mentioned; no case of tortuosity evolution was reported.

Our Sample. Increased artery tortuosity was detected in all children at any age. The finding was evident both on T2 parenchymal

imaging and MRA (On-line Fig 1). Both semiquantitative and quantitative basilar artery evaluation showed significantly increased tortuosity compared with age-matched controls ($P < .0001$; Table 1 and Fig 2) and no correlation with age. Children with MD with neuroradiologic follow-up showed no significant evolution of the basilar artery changes (Table 3).

Stenosis and ectasia of the intracranial arteries, though repeatedly mentioned in the literature as possible pathogenic mechanisms of parenchymal lesions,^{7,8} were never detected in any of the present children with MD or in those reported in the literature.

Widening of the venous sinuses, recently reported in 1 child with MD,⁷ was detected in 1/26 children in the present sample (On-line Fig 2A).

White Matter Changes: Tumefactive Lesions

Literature Review. At first MR imaging, white matter tumefactive lesions were detected in 21/62 children with MD (33%; mean age, 4.8 ± 1.9 months; range, 1.2–10 months); in 3/62 (5%), the lesions were absent (mean age, 4.5 months; range, 3.5–6 months), whereas in the remaining 38/62, this finding was not mentioned. In 5/21 cases, tumefactive lesions were not restricted to the temporal regions. At follow-up MR im-

Table 2: Demographics and main clinical data of our children with MD and of children with MD in the literature who underwent brain MRI

Demographics	Present Sample	Literature Review (On-line Appendix)
Sample size	26 Children	62 Children
Sex	25 M; 1 F	57 M; 5 F
Age at clinical onset (mean) (range) (mo)	3.7 ± 2.5 (1–8) ^a	4.5 ± 3.3 (0.1–14) ^b
Age at first MRI (mean) (range) (mo)	7.5 ± 5.9 (0.3–32.2)	7.1 ± 5.6 (0.6–34.0)
Follow-up MRI	8/26 Children	23/62 Children
Age at last follow-up (mean) (range) (mo)	25.3 ± 19.4 (3.6–86.7)	10.2 ± 6.28 (1.5–30)
Follow-up duration (mean) (range) (mo)	22.8 ± 23.1 (1.4–78.5)	6.1 ± 5.9 (0.3–26)
Epilepsy	23/26	37/62
Age at epilepsy onset (mean) (range) (mo)	6.5 ± 3.4 (2.2–15.0)	4.6 ± 3.3 (0.1–14) ^c

^a Calculated from 25/26 MD children.

^b Calculated from 31/62 MD children.

^c Calculated 19/37 MD children with epilepsy.

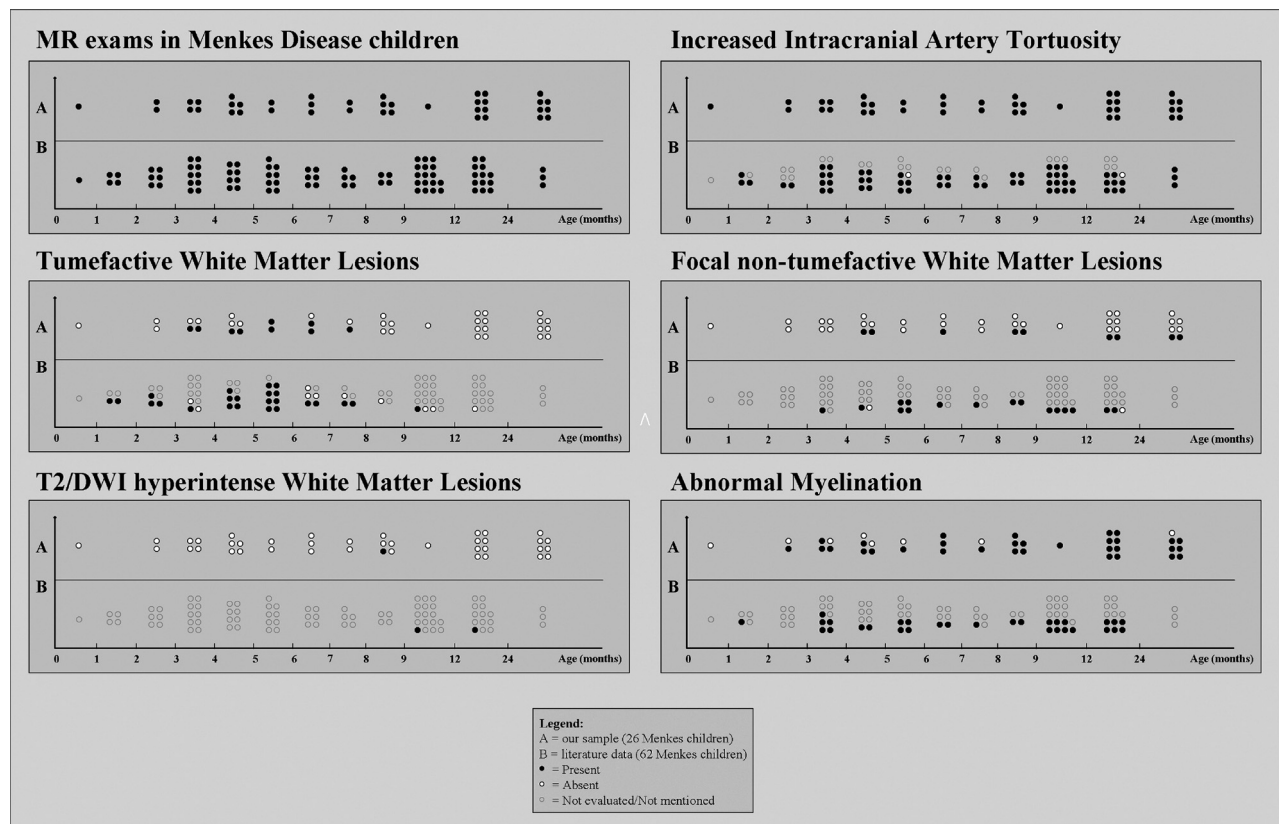


FIG 1. MR imaging findings in Menkes disease according to age at examination: A, Our sample (26 children, 40 examinations). B, Literature review (62 children, 86 examinations).

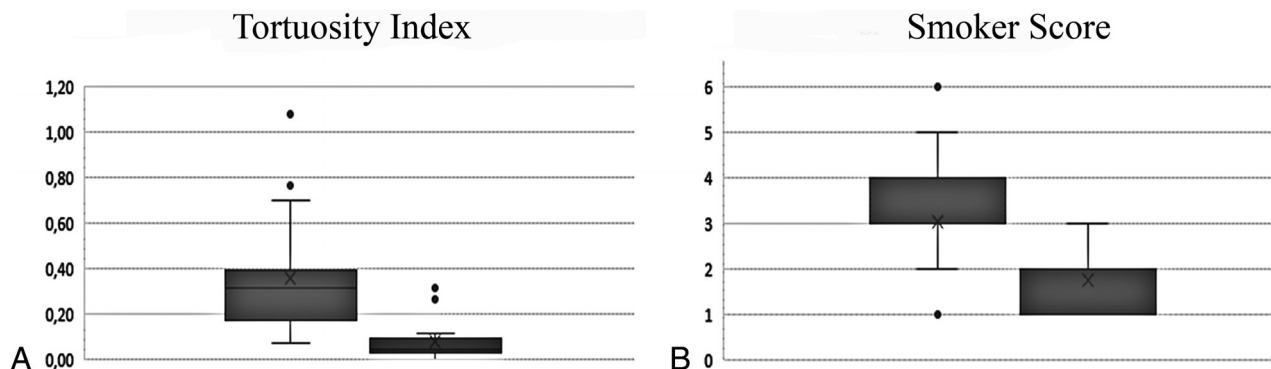


FIG 2. Tortuosity index (A) and Smoker score values (B) in children with MD (box on the left) and age-matched controls (box on the right). The difference was highly significant ($P < .0001$).

Table 3: Tortuosity index and Smoker score evolution among our MD children with MR follow-up

	First MR Exam	Last MR Exam
Tortuosity index	0.29 ± 0.11 (0.14–0.39)	0.26 ± 0.10 (0.14–0.32) ^a
Smoker score	3 ± 1.3 (1–6)	3.3 ± 0.7 (2–4) ^b

^a Obtained from 3 MD children with MRA follow-up (follow-up duration: 46.3 ± 30.3 months).

^b Obtained from 7 MD children with MRI follow-up (follow-up duration: 25.5 ± 25.3 months).

aging, tumefactive lesions were detected in 3/23 children (13%; mean age, 2.7 months; range, 1.5–4 months; in one child, the lesions were absent at first examination), were absent in 7/23 (30%) (mean age, 8.6 ± 2.9 months; range, 6–15 months; all had tumefactive lesions at first MR imaging), and were not mentioned in the remaining 13/23.

Our Sample. Tumefactive lesions were detected at first MR imaging in 7/26 (27%; mean age, 5.8 ± 1.3 months; range, 4.6–7.7 months; On-line Fig 3) and in 2 additional children with MD at follow-up MR imaging (both at 3.6 months of age). Among children with MD examined in the time window of 3–8 months, the detection rate was 9/16 (56%). In addition, among the 9 children with MD with tumefactive lesions, 2 had follow-up MR imaging and both showed full regression of the lesions. The presence of recurrent seizures or status epilepticus in the month preceding MR imaging was not associated with the detection of tumefactive lesions (6/9 versus 18/31 MRIs, nonsignificant, Fisher exact test). Temporal involvement was detected in all children with MD with tumefactive lesions (unilaterally in 1/9) and spread toward other lobes in 6/9 children (patients 5, 7, 9, 10, 16, and 26); the extra-temporal involvement was more frequent than that reported in the literature in children with MD (67% versus 23%, $P = .04$, Fisher exact test). Tumefactive lesions were distinctly asymmetric in 3/9.

All tumefactive lesions had strikingly T2-hyperintense subcortical white matter that appeared iso-hypointense on DWI with increased apparent diffusion coefficient values; the cortical ribbon did not appear involved despite sulcal effacement.

WM Changes: Centrum Semiovale DWI Hyperintense Lesions

Literature Review. Bilateral drop-shaped centrum semiovale lesions have been reported in 1/62 children with MD (1.6%) at 10

months of age; the lesions, hyperintense in DWI with restriction of water molecule movement, showed a size increase at 13-month follow-up.

Our Sample. Bilateral centrum semiovale lesions with identical signal features were detected in an 8-month-old child (3.9%, patient 6, On-line Fig 2B).

WM Changes: Focal Nontumefactive White Matter Lesions

Literature Review. Focal white matter lesions other than the tumefactive and DWI-hyperintense ones described above were detected at first MR imaging in 14/62 children with MD (23%; mean age, 7.2 ± 3.6 months; range 3–17 months) and were not mentioned in the remaining 48/62 children. At follow-up MR imaging, white matter focal lesions were present in 3/23 children with MD (13% not mentioned in previous examinations), absent in 2/23 (absent and not mentioned in previous examinations in 1 case each), and not mentioned in 18/23 (notably, 3 of them had lesions at first MR imaging, while in 15, the finding had not been mentioned).

Our Sample. Focal white matter lesions were detected in 9/26 children with MD (35%; mean age, 14.1 ± 11.0 months; range 4.6–32.7 months). Among the 8 patients with MR follow-up, 5 still had no lesions, 1 showed lesion regression, and 2 presented with new lesions.

Abnormal Myelination

Literature Review. Abnormal myelination was reported at first MR imaging in 20/62 children with MD (32%; mean age, 6.6 ± 3.9 months) and was not mentioned in the remaining 42/62 children. At follow-up, this finding was detected in 9/23 (39%) (in 4/9, it was not mentioned at previous MR imaging) and was not described in the remaining cases.

Our Sample. Abnormal myelination was found in 19/26 (73%; mean age, 8.7 ± 6.5 months; On-line Fig 4). Normal myelination was more frequently detected among earlier MRIs (especially younger than 6 months of age). In 1 child, the abnormal myelination appeared at follow-up at 15.6 months of age (the first MR imaging performed at 4.8 months showed normal myelination for age). Cases with longer follow-up MR imaging showed a progres-

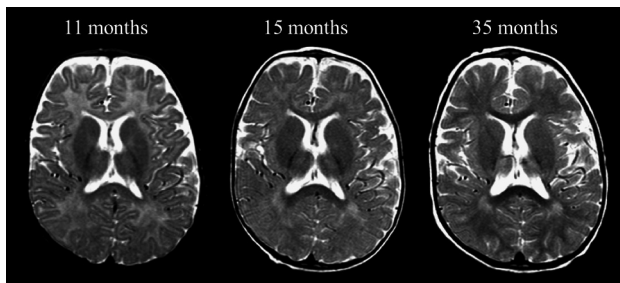


FIG 3. Axial T2-weighted images at the level of the genu/splenium of the corpus callosum in a boy (patient 8) affected by Menkes disease, showing the progressive-though-delayed supratentorial myelination.

sion of the myelination during the disease course (Fig 3). In the girl with MD, the myelination became normal at the last MR imaging (86.7 months of age).

Further Statistical Analyses

Possible associations among clinical data and parenchymal or vascular abnormalities were investigated, revealing a weak association between increased basilar artery tortuosity and white matter lesions, different from tumefactive lesions (0.56 ± 0.35 versus 0.24 ± 0.12 , $P = .02$), and a trend toward an association between earlier epilepsy onset and tumefactive lesions (4.9 ± 2.5 versus 7.6 ± 3.7 , $P = .07$) and between later clinical onset and white matter lesions, different from tumefactive lesions (4.9 ± 2.3 versus 3.2 ± 2.5 months, $P = .09$). No further significant associations were found among clinical and neuroradiologic findings (eg, tumefactive lesions versus status epilepticus or refractory seizures in the month preceding MR imaging examination, tumefactive lesions versus basal ganglia abnormalities, increased vascular tortuosity severity versus inguinal hernia, a marker of connective tissue laxity, or basal ganglia lesions; $P > .1$ in all cases).

DISCUSSION

The present retrospective cross-sectional multicenter study analyzed the neuroradiologic MR imaging abnormalities in children affected by Menkes disease, providing a detailed description of intracranial vascular and parenchymal changes in this rare disease. In this Part, we will address the most remarkable intracranial vessel and white matter MR imaging findings in our sample (26 children with MD) and the available literature (62 children with MD).

Intracranial Vascular Changes

Increased artery tortuosity is considered a typical diagnostic feature of Menkes disease, being reported in nearly 75% of cases and absent in <4% of cases. Nonetheless, it is still unclear whether this feature is progressive, eventually leading to blood supply abnormalities; stable since birth; or detectable even at a fetal stage, thus representing a useful prenatal diagnostic disease marker. Indeed, in the MD literature, abnormal intracranial artery tortuosity has sometimes been described only on follow-up examinations, thus suggesting a possible progression of artery changes. However, these case reports lacked a careful description of the anatomic conformation of the intracranial arteries at disease onset, leaving some uncertainty as to whether the tortuosity had truly appeared

at follow-up or had been overlooked at disease onset. In our sample, an increased tortuosity was a constant age-independent MD marker, thus confirming its important diagnostic role in the very first months of life. The youngest child with MD (patient 26), scanned in the neonatal period (20 days of life) for cutis laxa before neurologic onset, already showed the typical vessel changes. On the contrary, the lack of intracranial increased arterial tortuosity seems to make MD rather unlikely and should prompt reconsidering other diagnoses.

An increased tortuosity of the intracranial arteries was confirmed in our sample by both semiquantitative and quantitative basilar artery evaluations, which showed significant changes compared with age-matched subjects. Considering that the control group included children undergoing MR imaging/MRA for the suspicion of intracranial vascular problems, the difference is even more meaningful and confirms the major role of intracranial artery evaluation in the diagnostic work-up of MD. Regarding the evolution of the intracranial artery changes, the lack of association between age and both the tortuosity index and Smoker score at the cross-sectional evaluation and the lack of significant changes in children with MD undergoing MR imaging follow-up provide some evidence of early, most likely late-fetal or early-postnatal, vessel wall damage that remains relatively stable during the subsequent disease course. Intracranial artery elongation has been related to decreased activity of the copper-dependent lysyl oxidase, which is involved in elastin and collagen cross-linking, resulting in structural impairment of the blood vessel wall.⁹⁻¹⁵ Because during the whole intrauterine life, the circulating copper is provided by the mother, early vascular wall impairment points to a key role of *ATP7A* for lysyl oxidase function within the cell.¹⁶

The absence of intracranial artery ectasia and stenosis, either at onset or at follow-up, is another important result. Previous studies have reported possible ectasia or distal narrowing of intracranial arteries.^{7,8} Even though no imaging study directly has yet shown significant vessel lumen abnormalities, artery narrowing has been repeatedly advocated as a likely cause of ischemia and encephalomalacia. Actually, according to our experience (Online Fig 1C), the apparent distal artery caliber change was the result of artifacts related to the acquisition sequence used for investigating intracranial arteries. In fact, the commonly used MRA sequence (TOF) applies a saturation band just above the acquisition slab, aiming to cancel the cranial-caudal (venous) blood flow. The increased tortuosity of intracranial arteries can easily result in artery segments with downward-directed blood flow; the consequent artifactual signal loss might eventually lead to the false detection of stenosis and subsequent ectasia as the blood flow becomes again caudal-cranial. Indeed, the rare pathologic studies seem to confirm our neuroimaging findings, showing mild intima hypertrophy without significant abnormalities of vessel caliber and patency.⁶

Recently, dural sinus ectasia has been reported in a child with MD and has been suggested as a potentially interesting new disease marker.⁸ Indeed, this feature has also been detected in 1 child of our sample. Nonetheless, its low detection rate (1/26, 4%) raises some doubts about the real impact of venous changes and the utility of a dedicated evaluation of the intracranial venous system in the suspicion of MD.

Parenchymal Abnormalities

White Matter Tumefactive Lesions. In previous publications,¹⁷⁻¹⁹ tumefactive white matter lesions have been variably named “white matter cystic changes,”¹⁹ “leukoencephalopathy,”²⁰ and “transient edema of the temporal lobes.”²¹ All these lesions shared the following MR imaging features: The affected white matter presented striking T2-hyperintensity and increased ADC values consistent with vasogenic edema, the cortical ribbon was relatively spared, and the lesions had mild/moderate mass effect. Because data were derived almost exclusively from case reports, the frequency rate of tumefactive lesions in MD has not yet been defined. The present literature analysis points to a frequency rate slightly above one-third of children with MD, similar to that observed in our sample (37% versus 34%, respectively), thus suggesting that tumefactive lesions are usually not overlooked in routine conventional MRIs.

Tumefactive lesions may be uni- or bilateral, symmetric or asymmetric; most lesions are localized in the temporal lobes, disclosing the high vulnerability of these regions, especially the anterior portion (temporal pole). Nonetheless, involvement of other cerebral lobes is not uncommon: An extratemporal involvement was reported in nearly one-quarter of the children with MD with tumefactive lesions in the literature. In our sample, the detection of extratemporal lesions rose to two-thirds, most probably not because of differences between the 2 study populations but because of the different, more systematic approach at imaging evaluation.

One of the most interesting results of the present study is the identification of a specific age window for the appearance of tumefactive lesions. According to the literature review, children with MD presented with tumefactive lesions solely within the age range of 1.2–10 months (3–8 months in our sample). The recognition of a specific age window for tumefactive lesions implies the existence of an age-dependent brain vulnerability in MD that does not include the very early postnatal period and does not persist beyond the tenth month of life. Besides, the lack of detection of tumefactive lesions in children with MD undergoing MR imaging after 10 months of age suggests an evolution of those lesions that were detected in >50% of MRIs during the age window of 3–8 months. Indeed, the literature review,^{18,21} as well as 2 children with MD in our sample (patients 22 and 23), showed the reversibility of tumefactive lesions at follow-up MR imaging, raising some questions about their nature and pathogenesis.

In the past, some authors^{4,17,20,22} hypothesized for tumefactive lesions an ischemic pathogenesis that is not consistent with the currently available neuroradiologic findings because of the following: 1) Tumefactive lesions involve almost exclusively the white matter, sparing the contiguous cortex, while the latter is usually more vulnerable to ischemia; 2) DWI does not reveal cytotoxic edema, which, instead, characterizes ischemia; 3) tumefactive lesions do not respect vascular territories; and 4) tumefactive lesions seem to be reversible, while ischemic lesions are mostly irreversible and typically result in focal encephalomalacia.

Other authors suggested the existence of a pathogenic relationship between tumefactive lesions and refractory seizures or status epilepticus.^{17,18,20} A protracted epileptic activity might result in severe parenchymal edema, both vasogenic and cyto-

toxic.¹⁷ Vasogenic edema primarily derives from the persistent and severe brain acidosis associated with status epilepticus, eventually leading to blood-brain barrier alteration, parenchymal swelling, and sulcal effacement, while cytotoxic edema is likely due to the excessive neuronal stimulation with alteration of cell membrane permeability and neuronal/glial swelling. Postcritical cytotoxic edema usually prevails in the cortex,¹⁷ might spread to ipsilateral pulvinar and hippocampal formation, and has no or mild mass effect. Actually, tumefactive lesions did not show cytotoxic-like features in any children in the literature or our sample children with MD. In addition, in our relatively large sample, we were not able to replicate the hypothesized association between tumefactive lesions and the presence of status epilepticus or refractory seizures in the few days before MR imaging, even while restricting the analysis to within the temporal window in which tumefactive lesions have been detected (3–8 months). Taken together, these data do not support the hypothesis of a causal relationship between tumefactive lesions and excessive seizure activity. Most likely, tumefactive lesions and status epilepticus are simply independent epiphenomena of the same copper-related metabolic dysfunction.

DWI Hyperintense Centrum Semiovale Lesions. Although found in only 2 children with MD, considering both the literature and our sample, white matter cytotoxic-like lesions merit discussion due to their very peculiar MR imaging features. In both children with MD, these lesions had an oval or drop-like shape (On-line Fig 2B), were well recognizable on T2 images, but different from tumefactive lesions; they were located in the deep white matter and were strikingly DWI hyperintense with decreased ADC values. In the sole child with MD with follow-up MR imaging after 3 months, the lesions increased in size, maintaining a prevalent cytotoxic edema-like appearance. The pathogenesis of these lesions is still uncertain; the prolonged persistence of cytotoxic edema is not consistent with a brain infarct because the latter loses DWI hyperintensity within 1 month, evolving into focal encephalomalacia; in addition, the affected regions, both at onset and follow-up, did not correspond to a specific vascular territory. Most likely, centrum semiovale lesions are due to copper-dependent metabolic processes,²² leading to compromised mitochondrial function and eventually to a metabolic, not ischemic, stroke.

The very low frequency of DWI hyperintense lesions of the centrum semiovale in children with MD suggests the coexistence of environmental or genetic pathogenic factors, but it also hinders their identification. One of the 2 children with centrum semiovale lesions, for example, had a rare deletion of the exon 21, while in the other child, the genetics were not specified.

Focal Nontumefactive White Matter Lesions. According to our literature review, focal nontumefactive white matter lesions are reported in about one-fourth of children with MD, while the analysis of our sample showed a frequency rate slightly above 40%. Once again, the difference rate is most likely due to a more systematic search in our sample rather than to a true lower rate of focal nontumefactive white matter lesions in the literature data. These white matter lesions appear as T2/FLAIR-hyperintense/DWI-isointense regions, do not show a precise or restricted temporal occurrence, and present no specific morphologic pattern

(all lobes were variably involved in our sample). From the literature review, it was not possible to gain useful information about lesion evolution because follow-up data were lacking. In our sample, focal nontumefactive white matter lesions had a heterogeneous and unpredictable course, with lesions progressing during the disease course in most cases but also with 1 child who showed lesion regression at follow-up. According to some authors, focal white matter lesions stem from the progressive and diffuse cortical neurodegeneration and represent a secondary white matter degeneration.²³ However, this hypothesis does not explain why the lesions are focal, while neurodegeneration is more often a global phenomenon and focal cortical lesions are absent or present with regional inconsistency. In addition, our study did not reveal any association between these lesions and the presence or the severity of brain atrophy. According to other authors, these lesions would result from ischemic phenomena caused by vascular anomalies.^{1,4,7,8,19,22,24} The association between intracranial artery tortuosity and nontumefactive white matter lesions found in the present study seems to support a possible link between the processes leading to vascular wall abnormalities and white matter involvement. Nonetheless, because tortuosity changes do not seem to be associated with artery lumen changes, the ischemic hypothesis remains aleatory; moreover, focal white matter lesions do not cluster in specific vascular territories, and both the literature review and our sample analysis did not detect any lesion with DWI features of acute ischemia.

An alternative hypothesis suggested a relationship between white matter changes and the metabolic energetic failure due to copper-dependent enzymes.¹⁷ Similar white matter abnormalities have been observed in mitochondriopathies caused by deficiency of the cytochrome C oxidase enzyme,¹⁷ which is also impaired in MD and might result in brain cell death and demyelination. The present study was not powered for addressing this issue properly, but the extreme phenotypic variability of white matter lesions suggests that several pathogenic mechanisms are likely involved, leading to progressive white matter deterioration.

Abnormal Myelination. Abnormal myelination of the supratentorial white matter is a well-known finding in MD. It is present in about one-third of the literature MRIs and in more than two-thirds of our sample. Discrepancies in the detection rate most likely reside in the challenging discrimination between abnormal myelination both in early and in late phases of the disease course. In fact, brain myelination is physiologically incomplete in the first years of life, and its evaluation requires some expertise in pediatric neuroradiology. On the other hand, advanced phases of MD might present with superimposing neurodegenerative processes that imply diffuse gliosis/Wallerian degeneration with concomitant white matter signal abnormalities.

Notably, most children with MD have normal myelination at birth, suggesting that the lack of *ATP7A* function does not significantly influence myelin formation during fetal development, in contrast to what happens regarding vascular tortuosity that is abnormal even despite maternal-mediated copper absorption. Abnormal myelination is therefore diagnosed when the expected myelination milestones are not reached (eg, the anterior limb of the internal capsule at 6 months of age) and might become more evident with increasing age. Whether myelination abnormalities

were due to a halt or a delay in the myelination process, it appears unequivocally disentangled by the longitudinal MR imaging evaluation that, in our sample, repeatedly showed myelination progression (Fig 3) or even myelin full maturation at 7 years of age, though the latter child with MD was the female subject (patient 13), likely with a milder form of MD.



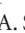


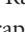
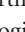
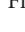

CONCLUSIONS

Intracranial vascular and white matter findings appear strikingly heterogeneous in Menkes disease. According to our data and literature review, a significantly increased arterial tortuosity seems to represent an early and reliable diagnostic biomarker of Menkes disease. On the other hand, there is no evidence of significant vessel wall change evolution during the disease course, and the role of artery changes in the pathogenesis of brain injury appears to be very weak, if present at all. Regarding the white matter involvement, myelin abnormalities seem to result from different, sometimes concomitant pathogenic mechanisms. Besides a delayed-but-improving postnatal myelination process, neurodegenerative phenomena implying gliosis and Wallerian degeneration might variably influence myelin signal. In addition, several heterogeneous focal lesions might occur, some of which seem to reveal a temporally selective white matter vulnerability during the course of Menkes disease.

ACKNOWLEDGMENTS

We thank the association “Angeli per la vita” and the Società Italiana di Neurologia Pediatrica, which strongly supported this spontaneous large Italian study.

The Menkes Working Group in the Italian Neuroimaging Network for Rare Disease includes the following members: Irene Toldo, Cinzia Peruzzi, Roberta Vittorini, Alberto Spalice, Carlo Fusco, Margherita Nosadini, Laura Farina, Alessandro Stecco, Gabriele Polonara, Maria Alice Donati, Lucio Giordano, Carlo Dionisi-Vici, Diego Martinelli, Aba Tocchet, Giuseppe Fariello, Francesco Nicita, Daniele Frattini, Paola Martelli, and Gaetano Cantalupo.

The following are collaborators in this work:  I. Toldo, Pediatric Neurology and Neurophysiology Unit, Department of Woman and Child Health, University Hospital of Padova, Padova, Italy;  C. Peruzzi, Child Neuropsychiatry, Ospedale Maggiore, Novara, Italy;  R. Vittorini, Child Neurology and Psychiatry, Department of Pediatrics and Pediatric Specialties, AOU Città della Salute e della Scienza, Torino, Italy;  A. Spalice, Children Neurology Division, University La Sapienza Roma, Italy;  C. Fusco, Child Neurology and Psychiatry Unit, Department of Pediatrics, ASMN-IRCCS, Reggio Emilia, Italy;  M. Nosadini, Pediatric Neurology and Neurophysiology Unit, Department of Woman and Child Health, University Hospital of Padova, Padova, Italy;  L. Farina, Department of Neuroradiology, Fondazione IRCCS Neurological Institute “C. Besta,” Milano, Italy;  A. Stecco, Unit of Neuroradiology, Institute of Radiology, Department of Diagnosis, Health Services and Therapy, “Maggiore della Carità” University Hospital-Novara, Novara, Italy;  G. Polonara, Clinica di Neuroradiologia, Dipartimento di Scienze Cliniche Specialistiche ed Odontostomatologiche; Università Politecnica delle Marche, Ancona, Italy; M.A. Donati, Metabolic Unit, A. Meyer Children’s Hospital, Firenze, Italy;

¹⁰L. Giordano, Child Neuropsychiatry Unit, “Spedali Civili,” Brescia, Italy; ¹¹C. Dionisi-Vici, Division of Metabolism, Bambino Gesù Children’s Hospital, IRCCS, Roma, Italy; ¹²D. Martinelli, Division of Metabolism, Bambino Gesù Children’s Hospital, IRCCS, Roma, Italy; ¹³A. Tocchet, Child Neurology and Psychiatry, Department of Pediatrics and Pediatric Specialties, AOU Città della Salute e della Scienza, Torino, Italy; ¹⁴G. Fariello, Ospedale Fatebenefratelli, Villa San Pietro, Dipartimento Immagini, Roma, Italy; ¹⁵F. Nicita, Department of Pediatrics and Child Neuropsychiatry, Child Neurology Division, Umberto I Hospital, Sapienza University of Roma, Roma, Italy; ¹⁶D. Frattini, Child Neurology and Psychiatry Unit, Department of Pediatrics, ASMN-IRCCS, Reggio Emilia, Italy; ¹⁷P. Martelli, Child Neuropsychiatry Unit, “Spedali Civili,” Brescia, Italy; ¹⁸G. Cantalupo, Child Neuropsychiatry Unit, Department of Surgical Sciences, Dentistry, Gynecology and Pediatrics, University of Verona, Verona, Italy; ¹⁹F. Zennaro, Institute for Maternal and Child Health-IRCCS “Burlo Garofolo,” Trieste, Italy.

Disclosures: Renzo Manara—UNRELATED: Payment for Lectures Including Service on Speakers Bureaus: Shire, Comments: about €1000.

REFERENCES

- Rizk T, Mahmoud A, Jamali T, et al. **Menkes disease presenting with epilepsy partialis continua.** *Case Rep Neurol Med* 2014;2014:525784 CrossRef Medline
- Tümer Z, Möller LB. **Menkes disease.** *European J Hum Genet* 2010; 18:511–18 CrossRef
- Nassogne MC, Sharrard M, Hertz-Pannier L, et al. **Massive subdural haematomas in Menkes disease mimicking shaken baby syndrome.** *Childs Nerv Syst* 2002;18:729–31 CrossRef Medline
- Bahi-Buisson N, Kaminska A, Nabbout R, et al. **Epilepsy in Menkes disease: analysis of clinical stages.** *Epilepsia* 2006;47:380–86 CrossRef Medline
- Van der Knaap MS, Valk J. *Magnetic Resonance of Myelination and Myelin Disorders Disorders.* Berlin: Springer; 2005
- Vuia O, Heye D. **Neuropathologic aspects in Menkes’ kinky hair disease (trichopolydystrophy): Menkes’ kinky hair disease.** *Neuropädiatrie* 1974;5:329–39 CrossRef Medline
- Bernhard MK, Merckenschlager A, Mayer T, et al. **The spectrum of neuroradiological features in Menkes disease: widening of the cerebral venous sinuses.** *J Pediatr Neuroradiol* 2012;1:121–25
- Gandhi R, Kakkar R, Rajan S, et al. **Menkes kinky hair syndrome: a rare neurodegenerative disease.** *Case Rep Radiol* 2012;2012:684309 CrossRef Medline
- Kaler SG, Holmes CS, Goldstein DS, et al. **Neonatal diagnosis and treatment of Menkes disease.** *N Engl J Med* 2008;358:605–14 CrossRef Medline
- Kaler SG. **ATP7A-related copper transport disease: emerging concepts and future trends.** *Nat Rev Neurol* 2011;7:15–29 CrossRef Medline
- Tang J, Donsante A, Desai V, et al. **Clinical outcomes in Menkes disease patients with a copper-responsive ATP7A mutation, G727R.** *Mol Genet Metab* 2008;95:174–81 CrossRef
- Danks DM, Campbell PE, Walker-Smith J, et al. **Menkes’ kinky-hair syndrome.** *Lancet* 1972;1:1100–02 Medline
- Danks DM, Cartwright E, Stevens BJ, et al. **Kinky hair disease: further definition of the defect in copper transport.** *Science* 1973;179: 1140–42 Medline
- Cosimo QC, Daniela L, Elsa B, et al. **Kinky hair, kinky vessels, and bladder diverticula in Menkes disease.** *J Neuroimaging* 2011;21: e114–16 CrossRef Medline
- Gu YH, Kodama H, Shiga K, et al. **A survey of Japanese patients with Menkes disease from 1990 to 2003: incidence and early signs before typical symptomatic onset, pointing the way to earlier diagnosis.** *J Inherit Metab Dis* 2005;28:473–78 Medline
- Royce PM, Camakaris J, Danks DM. **Reduced lysyl oxidase activity in skin fibroblasts from patients with Menkes’ syndrome.** *Biochem J* 1980;192:579–86 Medline
- Barnerias C, Boddaert N, Guiraud P, et al. **Unusual magnetic resonance imaging features in Menkes disease.** *Brain Dev* 2008;30: 489–92 CrossRef Medline
- Ito H, Mori K, Sakata M, et al. **Pathophysiology of the transient temporal lobe lesion in a patient with Menkes disease.** *Pediatr Int* 2008;50:825–27 CrossRef Medline
- Jain P, Sharma S, Sankhyan N, et al. **Macrocephaly with diffuse white matter changes simulating a leukodystrophy in Menkes disease.** *Indian J Pediatr* 2013;80:160–62 CrossRef Medline
- Bindu PS, Taly AB, Kothari S, et al. **Electro-clinical features and magnetic resonance imaging correlates in Menkes disease.** *Brain Dev* 2013;35:398–405 CrossRef Medline
- Ekici B, Çaliskan M, Tatli B. **Reversible temporal lobe edema: an early MRI finding in Menkes disease.** *J Pediatr Neurosci* 2012;7: 160–61 CrossRef Medline
- Johnsen DE, Coleman L, Poe L. **MR of progressive neurodegenerative change in treated Menkes’ kinky hair disease.** *Neuroradiology* 1991;33:181–82 CrossRef Medline
- Lee ES, Ryoo JW, Choi DS, et al. **Diffusion-weighted MR imaging of unusual white matter lesion in a patient with Menkes disease.** *Korean J Radiol* 2007;8:82–85 CrossRef Medline
- Lee J, Peña MM, Nose Y, et al. **Biochemical characterization of the human copper transporter Ctr1.** *J Biol Chem* 2002;277:4380–87 Medline